**Program Digest, 2019 IEEE International Ultrasonics Symposium (IUS)**
**Glasgow, Scotland, October 6-9, 2019**

# Characterization of Image-based Refocusing for Transcranial Therapies

P. D. O'Brien
*Electrical and Computer Engineering*
*University of Minnesota*
Minneapolis, USA
obrie844@umn.edu

Collin S. Smith
*Electrical and Computer Engineering*
*University of Minnesota*
Minneapolis, USA
smit8844@umn.eduT

Hasan Aldiabat
*Electrical and Computer Engineering*
*University of Minnesota*
Minneapolis, USA
aldia001@umn.edu

Dalong Liu
*Electrical and Computer Engineering*
*University of Minnesota*
Minneapolis, USA
liuxx293@umn.edu

Rajagopal N. Aravalli
*Electrical and Computer Engineering*
*University of Minnesota*
Minneapolis, USA
aravalli@umn.edu

Emad S. Ebbini
*Electrical and Computer Engineering*
*University of Minnesota*
Minneapolis, USA
ebbin001@umn.edu

***Abstract*—Transcranial focused ultrasound (tFUS) has the potential to provide precision ultrasonic targeting of brain circuits in the treatment neurological disorders. However, this potential is severely limited by FUS beam distortions through the skull. We have previously demonstrated the feasibility of using dual-mode ultrasound array (DMUA) capabilities to perform refocusing based on target identification on DMUA imaging. Furthermore, we have demonstrated improved refocusing when the target echoes are sufficiently coherent, as measured using a focusing data matrix (FDM) evaluated from raw channel data. The objective of this study is to characterize this geometric refocusing-aberration correction method and extend its use. Specifically, refocusing off of coherent echoes in the vicinity of the intended target as identified on DMUA imaging. *In vitro* transskull experiments were performed with sample skulls placed in the path of DMUA focused beams. Beam distortions were characterized using 2D hydrophone scans in planes orthogonal to the FUS beam axis before and after refocusing. The results provide experimental verification of the improved focusing gain achieved when refocusing at the target or points in its vicinity. The improvement was in the range of $3-7$ dB for a variety of target locations with respect to the skull suture lines.**

***Index Terms*—Transcranial FUS, Refocusing, Focusing Data Matrix**

## I. Introduction

Epilepsy is the fourth most common neurological disorder in the United States, affecting an estimated 2.2 million Americans in 2012 with an additional 150,000 new cases each year [1]. The most common treatments for Epilepsy include symptom management through drugs, surgical resection, vagal nerve stimulation, or a combination of treatments [2]. Precise delivery of transcranial focused ultrasound (tFUS) could act in combination with, or substitute for, each of the most common methods of epilepsy treatment. Precision is vital in treatment of Epilepsy and many others to ensure safe and effective treatment.

Funded by Grant NS098781 from the National Institute of Health

The precision tFUS application is currently limited by beam distortions caused by transmission through the skull. This limitation can be overcome with appropriate refocusing of the tFUS beam to copensate for distortions through the skull. Prada and Fink [3] introduced the DORT method, DORT being the French acronym for Decomposition of the Time Reversal property. The DORT-method measures the echo wave-field pattern of a collection of point-scatterers, decomposes the wave-field with an eigenvalue decomposition, and generates time-reversed transmission phase profiles for well-separated point-scatterers in the medium. This refocusing method is limited on two fronts. If the point-scatterers are not well-separated, then the eigenmodes do not strongly represent individual point-scatterers. Second, the operator does not define where the scatterer(s) are located in the tissue through imaging. Alternatively, the pseudoinverse method of pattern synthesis operates as an spatial equalization filtering process. Refocusing with the pseudoinverse operator began by refocusing ultrasound through the ribs to targets in the abdomen [ [4], [5]]. Both attempted to synthesize the wavefront from the target to the rib-cage, then propagate the field to the delivering aperture.

The first form of Image-based Refocusing was introduced in [6], which included the ability to refocus energy away from critical points in the imaging field of view. Imaging was used to select target and critical points, wherein the beamforming geometries were used to focus the energy or direct it away from critical points, in this case, the ribs.

The work described herein improves upon [6] by using the raw-channel imaging data to construct a Focusing Data Matrix (FDM) [7], which allows aberration correction in addition to controlling the tFUS wavefront to minimize incidence at critical points in the path of the beam. The FDM has previously been demonstrated to improve refocusing the target echoes when the target is sufficiently coherent. This work contains the first real-time demonstration of single transmit focus (STF) imaging for estimation of FDM and performing adaptive refocusing. In addition, the refocusing phase (delay) profiles are geometrically shifted to targets off of the dominant modes of the FDM.

The imaging and therapeutic performance of geometrically shifting the refocused profiles is compared to geometric targeting without any refocusing input. This should demonstrate the effectiveness of the aberration correction component of the proposed refocusing algorithm. Experimental results reported in this paper demonstrate the advantages of the refocusing approach compared to geometric focusing approach.

## II. Methods

### A. Imaging and Therapy System

*1) Dual-mode ultrasound array:* The ultrasound transducer is a 3.2 MHz, spherically focused (40mm radius of curvature), dual-mode ultrasound array (DMUA). The spherically-focused DMUA structure concentrates energy in a highly focused area, which can be used to perform reversible or irreversible, non-invasive ultrasound therapy. The same transducer which performs this therapy is also used to perform imaging, thereby making the transducer a dual-mode array. It can perform this imaging concurrently with therapy for treatment monitoring. The inherent 1-to-1 correspondence between the therapeutic and imaging beams could allow an imaging mode to act as a safe therapy performance predictor if both are similarly transmitted.

*2) Driver and Software Architecture:* The driving system the utilizes the capabilities of the DMUA through an inter-process communication, software-defined GPU-based beaformer, real-time, imaging and therapy platform. The system includes a multi-channel arbitrary waveform generator, which allows custom transmission waveforms for imaging and therapy modes. Additionally, it includes an adaptive imaging system, wherein transmission signals can be modified, updated, or changed in real-time based upon imaging feedback. The combination of all parts enables a real-time, closed-loop, adaptive, arbitrary transmission system to be implemented.

The work herein introduces the first real-time, adaptive, image-based refocusing scheme. The platform interrogates the target with a low-intensity imaging waveform, beamforms to create an image at speeds up to 500 frames per second (fps), generates focusing data matrices (FDMs) to measure the degree of defocusing, then updates the transmitted imaging and therapy waveforms with the most recent image-based refocusing phase profile to correct for defocusing. This process is can be repeated until convergence (i.e. no changes in refocusing driving waveforms) or feedback from the target region indicates therapeutic objectives have been met (e.g. real-time feedback includes focusing gain measurements). This use of the dual-mode capabilities of imaging and therapy can adapt to real-time changes in the target. In application, breathing motions, lesion growth, temperature changes, unexpected prefocal hot-spots, and many other treatment irregularities can be accounted and corrected for during treatments.

*3) Imaging Methods:* The system employs two primary modes of imaging that have been previously described [8]: synthetic aperture (SA) and single-transmit-focus (STF). SA imaging provides images useful for transcranial target identification and assisting in stereotaxic localization [9]. STF imaging is akin to the now widely used plane wave imaging, with the exception that the DMUA used herein is focused, often with the same focusing waveforms as the therapy beam. The objective is to estimate any significant scatterers in the path of therapy. Therefore, distortions or defocusing incurred during STF imaging mimics the distortion during therapy. If a target becomes brighter through image-based refocusing, it is expected that the therapeutic performance will be improved as well. Previous work demonstrated image-based refocusing of SA frames across multiple broadband frequencies while targeting specular structures; the work herein uses STF image-based refocusing for a faster, real-time, adaptive, ultrasound therapy monitoring solution [7].

### B. Experimental Setup

Wire targets and hydrophones are submerged in baths of degassed and deionized water to simulate transcranial structures. The skulls of Sprague Dawley rodents are placed in the beam path to distort the ultrasound beams. All skulls were harvested from animals used in other experiments; none were euthanized solely for this experiment. The Onda Corp. HNP-0200 hydrophone is used in the transskull hydrophone setup in Fig. 1 to measure the therapeutic performance of the image-based refocusing. A collection of 40 gauge wires are used to demonstrate the selective nature of image-based refocusing and target identification during imaging. Ultrasound images of these targets are taken with and without skulls in the beam-path to characterize the performance of image-based refocusing. A volume scan landmark visualization method defined in [9] allowed for consistent targeting of the same cranial windows across different skulls. In total, 6 different locations across 3 different skulls are examined. Both field scans and single-point intensity envelope measurements are taken to determine the therapeutic performance of the refocusing algorithm.

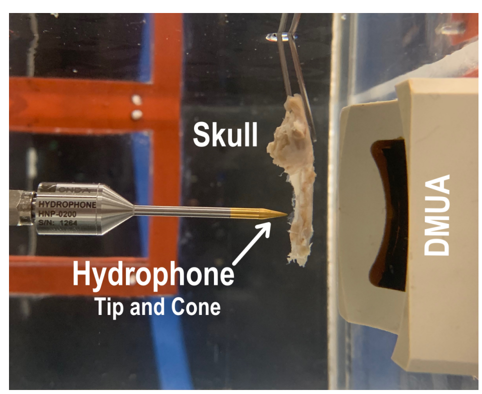


Fig. 1: Waterbath Hydrophone Experiment with Small Animal Skull

### C. Image-based Refocusing Algorithm

The image-based refocusing algorithm uses a focusing data matrix (FDM) to measure coherence and improve the coherence of specular targets within the tissue. In the work below, specular transcranial structures act as target points for refocusing and off-specular targets are targeted using the refocused profile with an additional geometric phase-shift. Critical points, discussed previously [10], are set at highly attenuation or distortion locations of the skull, such as suture lines, to direct transmission energy away from these problematic locations.

The FDM is constructed from echo data at both target and critical points to improve or reduce the specular coherence at these points respectively. An eigenvalue decomposition of the FDM is used to estimate the required aberration correction for a specular target. The resulting eigenmodes can represent individual specular targets or combinations of structures within the area defined by the FDM. Selecting individual modes will direct the following transmission towards the locations within the FDM the mode originated from. As discussed previously, the adaptive feedback system takes image frames during therapy, which can measure, and iteratively improve, the degree of refocusing for a given phase profile. When targeting a region away from the specular target, a geometric phase shift correction is added to the refocused profile for beamsteering away from specular targets. The imaging performance of the geometric shift adjustments are characterized through imaging results. The therapeutic performance away from specular targets is compared with and without the input of refocusing using hydrophone scans and point measurements.

## III. Results

### A. Wire Targets

Three wires located are used to demonstrate the effects of FDM mode-selection and target selection during refocusing. Figure 2 A) contains the depiction of the waterbath setup with three 40 guage wires, $W_{a,b,c}$, in a waterbath. Figure 2 B), C), and D) display enlarged, beamformed images using geometric targeting, targeting with a refocusing phase profile onto $W_b$, and targeting with a refocusing phase profile and geometric shift onto $W_c$. Initially, when using geometric targeting, the wire closest to the geometric focus, $W_a$, has the strongest echogenicity, while $W_b$ and $W_c$ suffer from diminished echogenicity. The pre-beamformed channel data used to generate Fig. 2 B) is used to form an FDM. Analyzing this FDM, it is seen that focusing information for targets $W_a$ and $W_b$ are strongly associated to unique modes, but the focusing information for wire $W_c$ is spread across a combination of nodes. Figure 2 C) shows the beamformed image using the phase profile from the mode focusing on $W_b$ for an imaging signal. As $W_b$ has become the strongest echogenicity source in Fig. 2 C), it can be surmised that this energy shift would occur in both the imaging and therapeutic beam. Fig 2 D) displays imaging with refocused eigenmode phase profile from $W_b$ onto the wire target $W_c$ using a geometric phase adjustment. 2 D) demonstrates a large energy shift in the imaging signal, and now can clearly identify $W_c$.

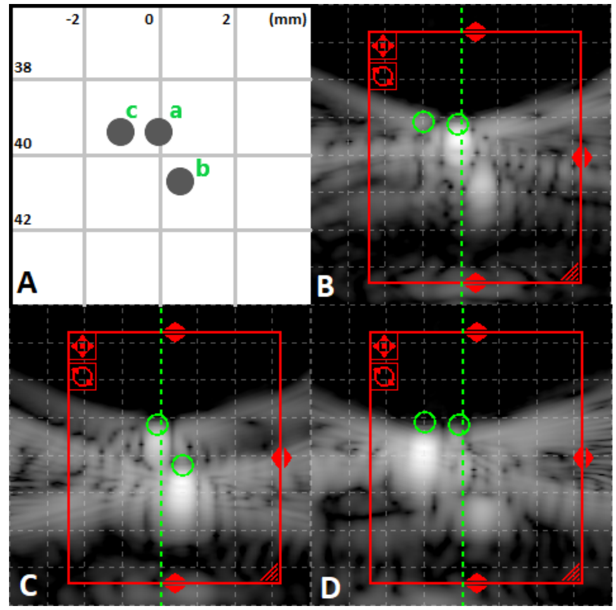


Fig. 2: Imaging 40 gauge Wire Targets using B) Geometric, C) Refocused, D) Refocused with Geometric-Shift Imaging Signals

Figure 3 displays the SA image of the hydrophone setup with additional overlays for demonstration. Fig. 3 displays two red overlays representing the −6 dB intensity areas geometrically targeting the green (specular target) and yellow (off-specular target). The blue overlays represent the −6 dB intensity areas targeting the green and yellow targets using image-based refocusing and image-based refocusing with a geometric-phase offset. Each intensity area was measured using a hydrophone field scan described below.

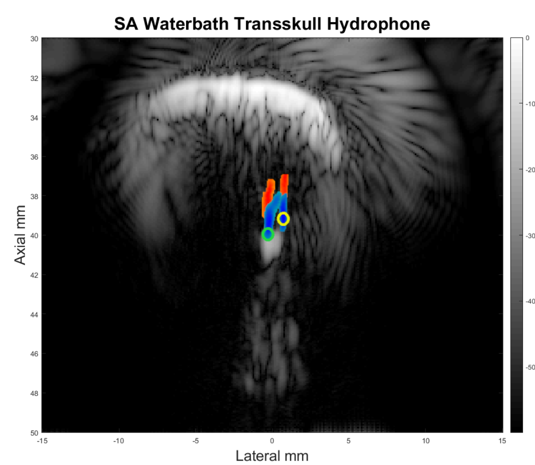


Fig. 3: Waterbath Hydrophone Experiment with Small Animal Skull

Geometric and refocused therapy profiles were transmitted transcranially and measured by the hydrophone. Example field scans measuring the geometric and refocused phase profiles are shown in Fig. 4. Each profile was attempting to target the white circles in 4, with the refocused phase profile clearly being the more accurate onto the target. These refocused phase profiles were then geometrically adjusted to target an off-specular target (yellow circle in 3) which rotated around the specular target (green circle in 3) for each skull and location. Fields scans were measured for each skull and location geometrically targeting the green and yellow targets, and were measured targeting using refocusing and refocusing with geometric-shifting to the green and yellow targets respectively.

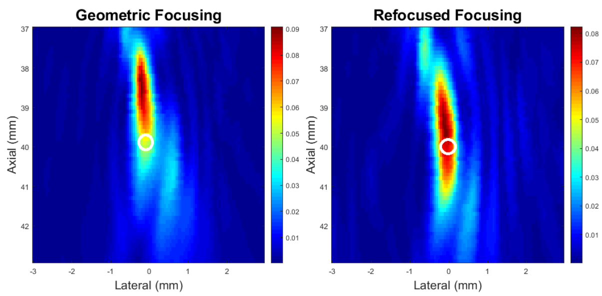


Fig. 4: Geometric vs Refocused Hydrophone Field Scan Transskull

The profile used to collect scans like Fig. 4 are also transmitted to measure hydrophone point measurements at the the targets in 3. Example intensity envelopes are shown in Fig. 5 for the specular and off-specular targets. Point measurements were collected for each skull and location.

Shown in the combined result Fig. in 3, a visible improvement of an approximately 1 mm in focus-shift correction and a smaller $-6$ dB area for both at and away from the coherent target. Results across the 6 different target locations from 3 skulls demonstrate an average of 1.78 mm focus shift error with an average refocusing correction of 1.06 mm. The yellow, speckle target was shifted around the coherent echo source both axially and laterally to collect these results, showing improvement each direction around the specular target.

Imaging also corresponded to the measured field scan results. The transskull specular targets increased in echogenicity by up to $+2.8$ dB. Measured therapeutic performance at the targets or in its vicinity increased between $3-6$ dB from geometric to refocused transmission. Furthermore, the critical points within the skull demonstrated reduced echogenicity by refocusing the energy away from that critical point. Reductions ranged from $-0.5$ to $-1.78$ dB. The off-specular targeting also decreased the specular targets echogenicity, directing more energy away from the original coherent source.

## IV. Conclusions

The image-based refocusing with geometric correction can more accurately deliver HIFU, with real-time adaptive updates, at and away from coherent targets. This work marks the first demonstration of a real-time adaptive image-based refocusing algorithm. Refocusing improves control of tFUS

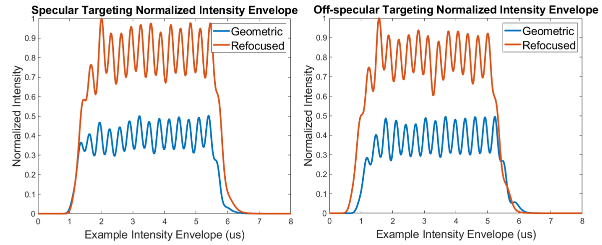


Fig. 5: Specular and Off-Specular Target Intensity Envelopes with or without Refocusing

therapies by: first, imaging with the refocused signals appears to predict therapeutic improvements. Second, it is capable of forming highly focused beams improving transkull therapeutic precision. Third, the intensity delivered to the target locations increased with refocusing at and away from specular targets. Finally, the adaptive nature of the image-based refocusing scheme can update the transmit therapy beam to account for shifts in the tissue, unpredictable pre-focal hot-spots, or developments in thermal or lesion-based therapies. This work opens the door for more confined treatment locations and greater control over therapeutic procedures within tFUS.

## References

[1] ”Epilepsy Across the Spectrum, Institute of Medicine, 2012.

[2] ”Epilepsy: Fact Sheet,” National Institutes of Health, June 30th, 2018.

[3] Claire Prada and Mathias Fink, ”Eigenmodes of the time-reversal operator: a solution to selective focusing in multiple-target media,” Wave Motion, vol. 20, no. 2, pp. 151163, 1994.

[4] Y. Botros, J. Volakis, P. Vanbaren, and E. Ebbini, A hybrid computational model for ultrasound phased-array heating in presence of strongly scattering obstacles, IEEE Transactions on Biomedical Engineering, vol. 44, no. 11, pp. 10391050, 1997.

[5] Y. Botros, J. Volakis, P. Vanbaren, and E. Ebbini, A hybrid computational model for ultrasound phased-array heating in presence of strongly scattering obstacles, IEEE Transactions on Biomedical Engineering, vol. 44, no. 11, pp. 10391050, 1997.

[6] J. Ballard, A. Casper, Y. Wan, and E. Ebbini, Adaptive Transthoracic Refocusing of Dual-Mode Ultrasound Arrays, IEEE Transactions on Biomedical Engineering, vol. 57, no. 1, pp. 93102, 2010.

[7] H. Aldiabat, P. O’Brian, D. Liu and E. S. Ebbini, ”Wideband Image-Based Transskull Refocusing Using Dual-Mode Ultrasound Arrays,” 2018 *IEEE International Ultrasonics Symposium (IUS)*, Kobe, 2018, pp. 1-4. doi: 10.1109/ULTSYM.2018.8579881

[8] A. J. Casper, D. Liu, J. R. Ballard and E. S. Ebbini, ”Real-Time Implementation of a Dual-Mode Ultrasound Array System: In Vivo Results,” in *IEEE Transactions on Biomedical Engineering*, vol. 60, no. 10, pp. 2751-2759, Oct. 2013. doi: 10.1109/TBME.2013.2264484

[9] D. Liu, K. Shiable, W. Low, and E. S. Ebbini, ”Three-dimensional image guidance for transcranial focused ultrasound therapy,” *Proceedings of the IEEE 14th International Symposium on Biomedical Imaging, April 18-21, 2017, Melbourne, Australia* [Electronic]. IEEE XPlore Digital Library, IEEE, 2017. https://ieeexplore.ieee.org/document/7950665. [Accessed: Aug. 30, 2019].

[10] Ballard, J. R., Casper, A. J., Wan, Y., and Ebbini, E. S. (2009). Adaptive transthoracic refocusing of dual-mode ultrasound arrays. IEEE Transactions on Biomedical Engineering, 57(1), 93-102.